

phate-labeled cRNA probes to *GDNF*, *Ret*, and *GFR- α 1* were as described [Z. Kokaia et al., *Eur. J. Neurosci.* **11**, 1202 (1999)]. The slides were exposed for 2 to 4 weeks and photographed with an Olympus Provis microscope equipped with a charge-coupled device camera (Photometrics, Munich, Germany). In the Adobe PhotoShop 4.0 program, the dark-field images were inverted, artificially stained red, and recombined with the bright-field images. The sense controls did not show grain density above background levels.

20. K. Yoshinaka et al., *Development* **113**, 689 (1991); B. H. Schrans-Stassen, G. J. van de Kant, D. G. de Rooij, A. M. M. van Pelt, *Endocrinology* **140**, 5894 (1999).

21. K. Yomogida et al., *Development* **120**, 1756 (1994).

22. The mice were injected intraperitoneally (ip) with BrdU (Amersham). After 2 hours, testes were dissected, fixed in Bouin, and processed in paraffin. BrdU incorporation was detected by monoclonal BrdU an-

tibody (Amersham) and indirect immunofluorescence [tetramethyl rhodamine isothiocyanate (TRITC) -antibody to mouse immunoglobulin G (IgG), 1:100; Jackson ImmunoResearch] or BSP labeling. Apoptotic cells were detected with the ApopTag kit (Intergen, Purchase, NY).

23. Electron microscopic biopsies were processed by standard methods and examined with a JEM 1200EX microscope (JEOL, Tokyo, Japan).

24. J. Widenfalk et al., *J. Neurosci.* **17**, 8506 (1997).

25. X. Meng and H. Sariola, unpublished data.

26. K. Akmal, J. Dufour, M. Vo, S. Higginson, K. Kim, *Endocrinology* **139**, 1239 (1998); T. Lufkin et al., *Proc. Natl. Acad. Sci. U.S.A.* **90**, 7225 (1993).

27. Wild-type and transgenic mice at 3 weeks of age ($n = 9$ mice in both groups) were injected ip with all-trans retinol (Sigma) (10 mg per kg of body weight per day). Testes were processed for histology after 3 or 8 days.

28. E. M. Eddy et al., *Endocrinology* **137**, 4796 (1996)

29. R. M. Pelletier and S. W. Byers, *Microsc. Res. Tech.* **20**, 3 (1992).

30. M. L. Meistrich and M. E. van Beek, in *Cell and Molecular Biology of Testis*, C. Desjardins and L. L. Ewing, Eds. (Oxford Univ. Press, Oxford, 1993), pp. 266-295; Y. Clermont, *Am. J. Anat.* **112**, 35 (1963).

31. E. F. Oakberg, *Am. J. Anat.* **99**, 391 (1956).

32. We thank A. Hanninen, K. Westerdahl, and P. Leikas-Lazanyi. K. Wartiovaara (University of Helsinki) cloned human GDNF cDNA. EE2 antibody was from Y. Nishimune (Osaka University, Japan). Supported by the Sigrid Jusélius Foundation, Technology Advancement Center of Finland (TEKES), the Academy of Finland, and EUBioMedII (contract BMH 4-CT97-2157).

3 November 1999; accepted 12 January 2000

General Acid-Base Catalysis in the Mechanism of a Hepatitis Delta Virus Ribozyme

Shu-ichi Nakano, Durga M. Chadalavada, Philip C. Bevilacqua*

Many protein enzymes use general acid-base catalysis as a way to increase reaction rates. The amino acid histidine is optimized for this function because it has a pK_a (where K_a is the acid dissociation constant) near physiological pH. The RNA enzyme (ribozyme) from hepatitis delta virus catalyzes self-cleavage of a phosphodiester bond. Reactivity-pH profiles in monovalent or divalent cations, as well as distance to the leaving-group oxygen, implicate cytosine 75 (C75) of the ribozyme as the general acid and ribozyme-bound hydrated metal hydroxide as the general base in the self-cleavage reaction. Moreover, C75 has a pK_a perturbed to neutrality, making it "histidine-like." Anticooperative interaction is observed between protonated C75 and a metal ion, which serves to modulate the pK_a of C75. General acid-base catalysis expands the catalytic repertoire of RNA and may provide improved rate acceleration.

Eight different catalytic RNAs (ribozymes) occur in nature, and all catalyze phosphoryl transfer reactions (1, 2). The rate of phosphoryl transfer can be accelerated by numerous factors, including stabilization of unfavorable charge development in the transition state, positioning of atoms, and ground-state destabilization (3). Developing negative charges in the transition state of the *Tetrahymena* ribozyme are stabilized by direct interaction with metal ions (4). Because the nucleophile must be deprotonated and the leaving group protonated, proton transfer must occur during phosphoryl transfer. Thus, developing negative and positive charges could, in principle, be stabilized by partial proton transfer in the transition state by general acid-base catalysis (2, 5, 6). Optimal proton transfer in enzymes occurs with an atom having a pK_a near neutrality (5, 6). Thus, histidine often plays an important role in

proton transfer in protein enzymes (5, 6).

In RNA, adenine and cytosine have the potential for protonation of their ring nitrogens N1 and N3, respectively, but the pK_a s for the free nucleosides are relatively low at 3.5 and 4.2 (7). Perturbation of adenine and cytosine pK_a s to near neutrality has been observed in several different RNAs (8-10), which suggests that effective acid-base catalysis may be possible in RNA. Imidazole rescue experiments have shown that proton transfer is possible in RNA catalysis and occurs in the hepatitis delta virus (HDV) ribozyme cleavage mechanism (10). The work described herein involves further characterization of the mechanism for this ribozyme.

HDV is a human pathogen that uses a ribozyme in its replication cycle (11). The ~85-nucleotide HDV ribozyme is found as closely related genomic and antigenomic versions (11, 12), and it belongs to a class of small ribozymes that produce cleavage products with 5'-hydroxyl and 2',3'-cyclic phosphate termini (1) (Figs. 1 and 2).

To probe the catalytic mechanism of the

HDV ribozyme, we examined the pH dependence for self-cleavage of the precursor genomic ribozyme, with a wild-type cytosine at position 75 (C75). The logarithm of the observed rate constant increases with pH between 4.5 and 6 with a slope of ~1 (Fig. 3A). In the pH range 7 to 9, the observed rate constant is pH insensitive, providing an observed pK_a of 6.1 in 10 mM Mg^{2+} (Fig. 3A). The slope of 1 at low pH is consistent with an increase in the concentration of the functional unprotonated form of one general base with pH and a constant amount of the functional protonated form of a general acid. The slope of zero from pH 7 to pH 9 indicates that either the concentrations of the functional species do not change with pH, or the concentration of one species increases while the other decreases by the same amount. To test the nature of the rate-limiting step, we conducted a solvent deuterium isotope experiment (Fig. 3A). A substantial D_2O solvent isotope effect [$= k_{max}(H_2O)/k_{max}(D_2O)$] was observed throughout the pK_a range 5 to 8, which suggests that the observed pK_a of 6.1 reflects a real ionization rather than a change in the rate-limiting step.

The crystal structure of the self-cleaved form of the genomic HDV ribozyme has been solved (13) and reveals that N3 of cytosine 75 (C75) is located only 2.7 Å from the 5'-oxygen of G1 (Figs. 2 and 3B). Moreover, biochemical data suggest that the precursor, transition state, and self-cleaved forms of the ribozyme have similar structures (13). Because the 5'-oxygen of G1 is the leaving-group oxygen in the self-cleavage reaction, C75 could serve as the general acid during self-cleavage (Fig. 2). To test this hypothesis, we replaced C75 with adenine (C75A) or uracil (C75U). The C75U mutant did not result in detectable self-cleavage (14). In contrast, C75A did react, albeit more slowly (by a factor of 270), resulting in an observed pK_a of 5.7 and a ΔpK_a of -0.4 compared with C75 (Fig. 3A). A pK_a shift of -0.4 is consistent with the unperturbed ΔpK_a for N1 of adenosine and N3 of cytidine of -0.65

Department of Chemistry, Pennsylvania State University, University Park, PA 16802, USA.

*To whom correspondence should be addressed. E-mail: pcb@chem.psu.edu

REPORTS

(the difference between 3.52 and 4.17) (7), which suggests that N3 of C75 participates in proton transfer. A similar ΔpK_a was recently observed for the analogous mutant (C76A) in the antigenomic ribozyme (10), which implies that this cytosine has the same mechanistic role in both ribozymes. In the crystal structure, the N4 amino group of C75 engag-

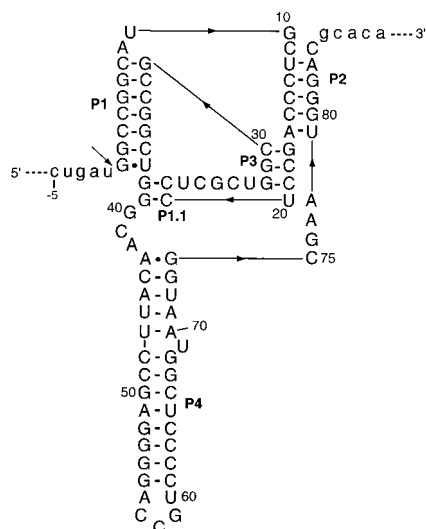


Fig. 1. Secondary structure of the HDV genomic ribozyme, based on the crystal structure of the self-cleaved form (13). Ribozyme sequence is in uppercase; flanking sequence is in lowercase. Base pairs and wobble pairs are denoted by dashes and dots, respectively. Pairings are denoted P, and representative nucleotides are numbered. Lines with internal arrowheads denote covalent linkages in a 5'-to-3' directionality. The G11C change present in all ribozymes is shown (33), and position 85 is a G (34). The cleavage site between u-1 and G1 is denoted with an arrow.

es in hydrogen bonding with the pro- R_p oxygen of C22 (Figs. 2 and 3B), which may be important for positioning C75 and perturbing its pK_a (13). The potential for this interaction as well as protonation of a similarly positioned ring nitrogen is maintained in C75A but not C75U. Also, the uracil mutants can be rescued by imidazole, supporting a role for proton transfer by C75 (10, 15). Lastly, in the pD profile, the pK_a is shifted upward by $\sim +0.4$ pH units (Fig. 3A), consistent with proton transfer by a ring nitrogen, because ammonium groups have typical pK_a shifts of $\sim +0.6$ pH units (16).

There are two distinct models involving C75 in proton transfer that could lead to the observed pH-reactivity profile for self-cleavage (Fig. 3A) (6). In model 1, C75 acts as the general base and ionizes near pH 7, and a general acid with $pK_a > 9$ participates in the reaction. In model 2, C75 acts as the general acid and ionizes near pH 7, and a general base with $pK_a > 9$ participates in the reaction. The pH-independent regime in model 2 is a consequence of the unprotonated general base concentration increase canceling out the protonated general acid concentration decrease. The major drawback of model 1 is that although the acid is in the functional protonated form near pH 7, it is weak. The major drawback of model 2 is that although the base is strong, it is mostly in the nonfunctional protonated form near pH 7. Linear free energy relationships on phosphodiester model compounds reveal large negative values for Brønsted $\beta_{\text{leaving group}}$ (≈ -1 to -1.3) (17). A large negative value for $\beta_{\text{leaving group}}$ indicates substantial development of negative charge on the 5'-oxygen atom of the leaving group in the uncatalyzed transition state.

Charge buildup can be neutralized by partial proton donation in the transition state from a general acid (18). Proton donation is favored by model 2 involving an acid with an optimal pK_a of 7, and disfavored by model 1 involving an acid with $pK_a > 9$.

In an effort to identify the general base, we examined the role of metal ions in self-cleavage. A hydrated alkaline earth metal hydroxide, represented as $[M(OH)]^+$, is a candidate for the general base because these species have pK_a 's > 9 (19). Prior studies indicated that the HDV ribozyme cleaves with a variety of alkaline earth and transition metal hydrates (20). We performed self-cleavage reactions in the presence of 10 mM $[\text{Co}(\text{H}_2\text{O})_6]^{2+}$ or 10 mM $[\text{Co}(\text{NH}_3)_6]^{3+}$, pH 7.0. Self-cleavage in $[\text{Co}(\text{H}_2\text{O})_6]^{2+}$ was complete in ~ 15 min, whereas no self-cleavage was detected with $[\text{Co}(\text{NH}_3)_6]^{3+}$ even after 24 hours (14). This contrasts with the hairpin ribozyme, in which $[\text{Co}(\text{NH}_3)_6]^{3+}$ can catalyze cleavage at a rate similar to that seen with hydrated divalent metals (21). Moreover, we found that $[\text{Co}(\text{NH}_3)_6]^{3+}$ inhibits the Mg^{2+} -catalyzed reaction in a competitive fashion; this suggests that $[\text{Co}(\text{NH}_3)_6]^{3+}$ binds to the same site as the functional magnesium ion but does not ionize (22). The $[\text{Co}(\text{NH}_3)_6]^{3+}$ complex is exchange-inert ($k_{\text{exchange, NH}_3} \approx 10^{-10} \text{ s}^{-1}$), which suggests that it binds through outer-sphere coordination (23).

Because $[\text{Co}(\text{NH}_3)_6]^{3+}$ and $[\text{Mg}(\text{H}_2\text{O})_6]^{2+}$ have similar size and geometry (21), we suggest a model in which the functional magnesium ion binds via outer-sphere coordination and ionizes to form a hydrated metal hydroxide $[\text{Mg}(\text{H}_2\text{O})_5(\text{OH})]^+$ that acts as the general base. Crystallographic studies of the *Tet*-

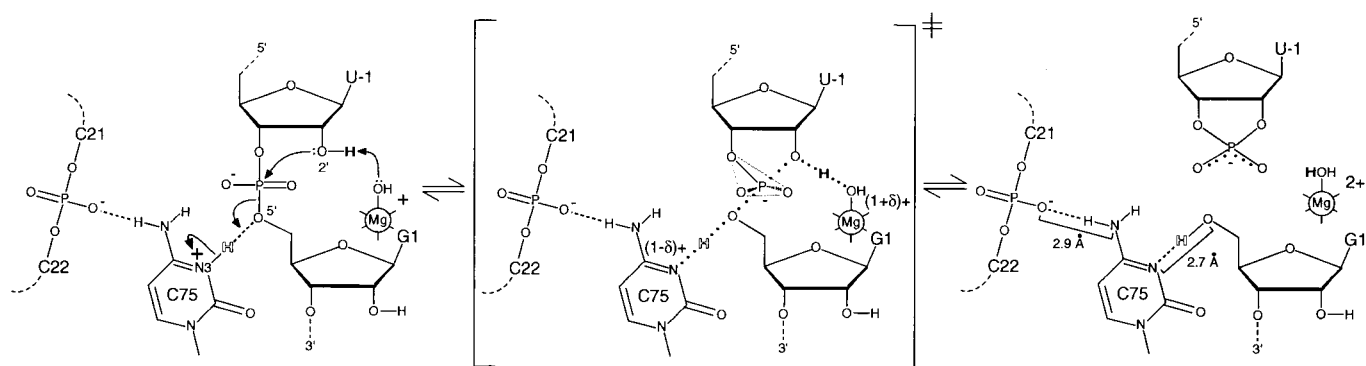


Fig. 2. Proposed mechanism for general acid-base catalysis in the HDV ribozyme. The scissile bond connects phosphorus and the 5'-oxygen of G1. The 2'-oxygen nucleophile is deprotonated (proton is bold H) in the precursor by a hydrated magnesium hydroxide, $[\text{Mg}(\text{OH})]^+$, acting as a general base, and the 5'-oxygen of the leaving group is protonated (proton is outline H) by C75 acting as a general acid. The reaction is drawn with a trigonal bipyramidal transition state based on parsimony. The 2'- and 5'-oxygens are drawn as neutral species in the transition state, as is typical for general acid-base catalysis (5). Redistribution of the charges on protonated C75 and $[\text{Mg}(\text{OH})]^+$ during the reaction is indi-

cated. In the transition state, the " δ " for loss of charge on C75 may be larger than the " δ " for gain of charge on the magnesium species, based on large values for Brønsted $\beta_{\text{leaving group}}$ (≈ -1 to -1.3) (17); if so, charge must be distributed to other atoms such as the equatorial oxygens. Distances are derived from the crystal structure of the self-cleaved form of the genomic ribozyme; the coordinate error of the structure was 0.3 to 0.4 Å (13). Hydrogen-bonding interactions in the precursor (depicted with dashed lines) were inferred from the structure of the self-cleaved ribozyme, because the two are believed to have similar structures (13).

REPORTS

rahymena ribozyme revealed that the major groove of tandem GU wobble base pairs forms a binding site for metal hexamines and metal hydrates (24). The genomic and antigenomic ribozymes contain a conserved GU wobble pair (the only GU in the ribozyme) at the cleavage site involving G1, for which the major groove face of G1 has been shown to be more important for function than the minor groove face (11). Examination of the crystal structure (13) reveals that the major groove of the G1U wobble pair is available for binding, and the major grooves of other guanines and phosphate oxygens are nearby and could act as hydrogen bond acceptors in outer-sphere metal binding. Studies on the HDV antigenomic ribozyme self-cleavage of a 2',5'-phosphodiester linkage also support a critical role for a metal ion at the cleavage site (25).

To examine the mechanism further, we tested for self-cleavage of the ribozyme in the absence of divalent metal. Self-cleavage in monovalent cations was observed in the presence of high ionic strength (0.5 to 2 M NaCl and 1 mM EDTA), and the rate in 1 M NaCl and 1 mM EDTA (pH 5.0) was approximately equal to that in 0.9 mM Mg²⁺ (pH 5.0) (Fig. 4, A and B, and Fig. 5A). Strikingly, in the pH range 6 to 8, the logarithm of the observed rate constant now decreases with pH, with a slope of ~ -1 (Fig. 4, A and B) (26). The pH dependence of the reaction is consistent with a decrease in the concentration of the functional protonated form of one general acid with pH, and is consistent with a constant amount of the functional unprotonated form of a general base (27). Reaction in 1 M NaCl and 1 mM EDTA was observed with C75 but not with C75U (14), which indicates that the general acid role of C75 in the transition state is unlikely to be changed in the absence of magnesium. Removal of the hydrated metal-hydroxide general base from the reaction unmasks the underlying general acid catalysis, providing direct functional evidence in support of model 2 in which C75 acts as the general acid and [M(OH)]⁺ as the general base (Fig. 2). High concentrations of monovalent cations substitute for magnesium ions in the tertiary folding of several RNAs (28). Self-cleavage of the HDV ribozyme in the absence of divalent cations suggests that divalent cations are not absolutely essential for folding or cleavage of the HDV ribozyme. However, inversion of the pH profile upon adding magnesium to the solution (Fig. 4A) strongly suggests that a functional magnesium ion does participate in the cleavage reaction under physiological conditions.

According to model 2, the observed pK_a for self-cleavage in divalent metal-containing reactions (e.g., Fig. 3A) is that of the general acid, C75. The reaction was examined in the presence of 10 mM concentrations of two

metals with different pK_as, Mg²⁺ and Ca²⁺. The unperturbed pK_a of a water molecule coordinated to Mg²⁺ is 11.4, and that for a water molecule coordinated to Ca²⁺ is 12.8 (19). Observation of similar pK_as of 6.1 and

6.3 in Mg²⁺ and Ca²⁺, respectively (Fig. 4A), is consistent with the observed pK_a for self-cleavage being that of the general acid C75 rather than the general base [M(OH)]⁺. The observed rate constant is slightly greater

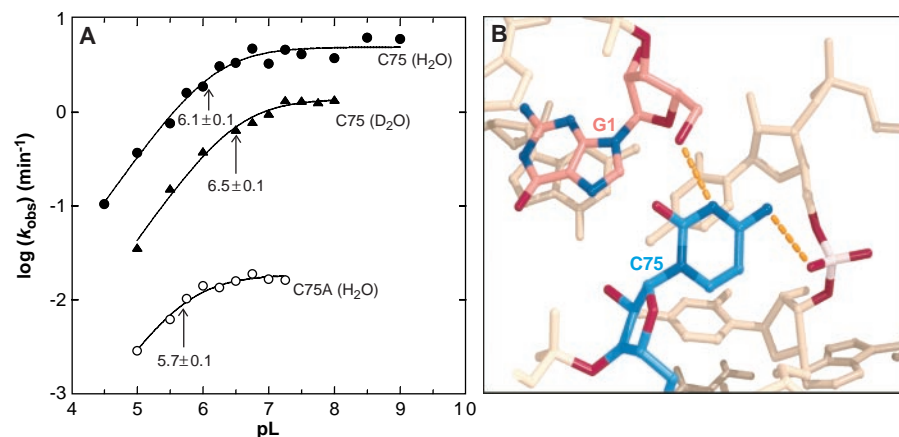


Fig. 3. (A) Reactivity-pH (-pH or -pD) profiles for C75 in H₂O (●), C75 in D₂O (▲), and C75A in H₂O (○). Both ribozymes contain a G11C change, which is a fast-folding ribozyme that reacts according to a single exponential (33). C75 refers to a ribozyme that contains a wild-type cytosine at position 75. Genomic ribozyme extends from positions -30 to 99 (34). Data were well fit by the single-exponential equation $y = A + B \exp(-k_{\text{obs}}t)$ using KaleidaGraph (Synergy Software), where k_{obs} is the observed rate constant for self-cleavage. The extent of reaction was at least 90% for the C75 ribozyme. The endpoint for C75A was maximal at pH 6 at $\sim 70\%$. The observed pK_a values were determined by fitting to the equation $k_{\text{obs}} = k_{\text{max}}/[1 + 10^{(\text{pK}_a - \text{pH})}]$ (5), and are given in the figure. The D₂O experiments were similar to the H₂O experiments with the following exceptions: The buffer was made in D₂O, and its pD was calculated by adding 0.4 to a pH meter reading (16). All the other reagents were dried in vacuo and dissolved in 99.9% D₂O (repeated once). **(B)** View of the active site of the self-cleaved form of the genomic ribozyme (73). G1 is shown in dark pink, C75 in light blue, and the phosphate bridging C21 and C22 in light pink. Nitrogen and oxygen atoms at these positions are colored blue and red, respectively. Hydrogen-bonding interactions important for general acid catalysis by C75 are as in Fig. 2 and are denoted by yellow dashed lines. [Produced with MIDAS (35).]

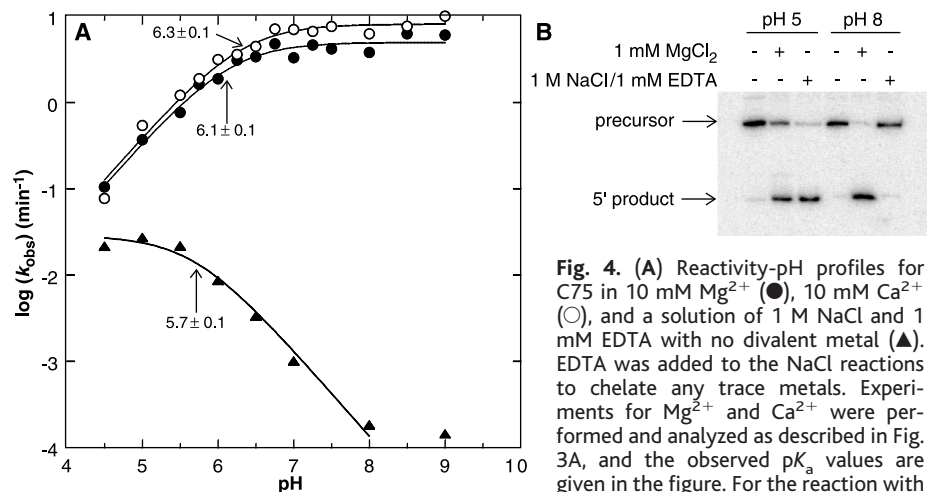


Fig. 4. (A) Reactivity-pH profiles for C75 in 10 mM Mg²⁺ (●), 10 mM Ca²⁺ (○), and a solution of 1 M NaCl and 1 mM EDTA with no divalent metal (▲). EDTA was added to the NaCl reactions to chelate any trace metals. Experiments for Mg²⁺ and Ca²⁺ were performed and analyzed as described in Fig. 3A, and the observed pK_a values are given in the figure. For the reaction with 1 M NaCl and 1 mM EDTA, quenching at various time points was done with 20 mM EDTA and 90% formamide; the products were immediately frozen on dry ice and stored at -20°C until needed. The data for 1 M NaCl and 1 mM EDTA were well fit by $y = A + B \exp(-k_{\text{obs}}t)$, and the fit went through the origin. The data at pH 8.0 and 9.0 were fit according to the initial velocity approximation $y = k_{\text{obs}}t$, using only the first 30% of the reaction. The observed pK_a value at 1 M NaCl and 1 mM EDTA was determined by fitting the data for pH 4.5 to 8.0 to the equation $k_{\text{obs}} = k_{\text{max}}/[1 + 10^{(\text{pH} - \text{pK}_a)}]$, and is given in the figure. **(B)** Self-cleavage in monovalent and divalent ions at different pH values after 2 hours of reaction at 37°C. Products were separated on a 10% denaturing polyacrylamide gel. The reaction with 1 mM MgCl₂ results in 0.87 mM free Mg²⁺ because of the presence of 0.13 mM EDTA in the solution.

REPORTS

in Ca^{2+} than in Mg^{2+} at $\text{pH} \geq 5$ (Fig. 4A). In contrast, the cleavage rate in the hammerhead ribozyme is faster in Mg^{2+} than in Ca^{2+} by a factor of ~ 16 (19), and this has been used to suggest direct interaction of the metal (acting as a Lewis acid) with a negatively charged oxygen atom in the hammerhead (2, 29). Similar observed rate constants in Ca^{2+} and Mg^{2+} (Fig. 4A) are consistent with a hydrated metal ion acting as a Brønsted base rather than a Lewis acid in the HDV ribozyme.

The nature of the pK_a shift for C75 was probed by measuring the pH dependence of the observed rate constant at different Mg^{2+} concentrations (Fig. 5A). The low-pH portions of the plots have slopes of ~ 1 , consistent with model 2 involving a single deprotonation of a metal-coordinated water molecule. The observed pK_a for C75 increases as the Mg^{2+} concentration decreases (Fig. 5A), indicating that a negative linkage exists between H^+ and Mg^{2+} binding. Indeed, the observed magnesium dissociation constant $K_{D,\text{Mg}^{2+}}$ decreases as pH increases (Fig. 5B), as required by detailed balancing, and Hill analysis is consistent with one functional magnesium ion binding between pH 4.5 and 8.0 (Fig. 5B). Linkage between H^+ and Mg^{2+} contrasts with the mechanism for the hammerhead ribozyme, in which H^+ and Mg^{2+} affect the cleavage rate independently (19), and supports close proximity of C75 and magnesium ion. At physiological Mg^{2+} concentrations of ~ 1 mM (30), the observed pK_a of C75 is near 7 (Fig. 5A), which is

optimal for general acid catalysis. At physiological pH of ~ 7 , the observed $K_{D,\text{Mg}^{2+}}$ is 2.4 mM (Fig. 5B), which is near the physiological concentration of Mg^{2+} (30). These observations suggest that the rate is optimized for physiological conditions.

The anticooperative interaction between protonated C75 and magnesium is electrostatic in nature, which can lead to large coupling in binding. In saturating Mg^{2+} of 50 mM, the pK_a is 5.8 (Fig. 5A). In low Mg^{2+} of 0.07 or 0.17 mM Mg^{2+} , the increase in the observed rate constant through pH 8.0 (Fig. 5A) suggests that C75 is still mostly protonated at pH 8.0, requiring a $\text{pK}_a \geq 8$ for C75. This provides a pK_a shift of at least -2.2 units due to metal binding, which gives a significant Gibbs free energy ΔG° for coupling of $\geq +3.1$ kcal/mol at 37°C . The pK_a shift for C75 in low Mg^{2+} concentration is ≥ 4 units from unperturbed cytosine, and may be due to favorable electrostatic interaction with the phosphate bridging C21 and C22 (13) and/or the scissile phosphate (Figs. 2 and 3B), as well as electron donation from N4 of C75. Indeed, similarly large pK_a shifts have been noted for proteins (31) and for a cytosine in a selected RNA (8). Unfavorable coulombic interactions between protonated C75 and bound $[\text{Mg}(\text{H}_2\text{O})_5(\text{OH})]^+$ should be partially relieved in the transition state because of charge redistribution (Fig. 2), which suggests that ground-state destabilization may provide a driving force for cleavage. In high concentrations of Na^+ , the observed pK_a is 5.7 (Fig.

4A); because this value is similar to the observed pK_a in 50 mM Mg^{2+} , monovalent cations in 1 M NaCl may be near the active site. Apparently, the positioning of charges in the binding cavity can substantially modulate the pK_a of a base.

Previous reports suggested that C75 (or its C76 analog in the antigenomic ribozyme) may be the general base in the self-cleavage reaction (10, 13). Likewise, the data presented here support a role for C75 in proton transfer, but they suggest that C75 is the general acid in the self-cleavage reaction. Paradoxically, C75 becomes optimized for general acid catalysis by a pK_a shift that makes it more basic, as this allows a greater fraction of C75 to exist in the functional protonated state at neutral pH. Moreover, in the presence of divalent metal, the observed rate constant increases with pH and reaches a plateau (Figs. 3A, 4A, and 5A), yet the observed pK_a for self-cleavage is that for a general acid rather than for a general base.

The ability of the HDV ribozyme to effectively carry out general acid-base catalysis under physiological conditions appears to be unique among known ribozymes (1, 2, 4). The extrapolated rate constant for the chemical step in the HDV ribozyme exceeds that for the *Tetrahymena* ribozyme and may approach the rate constant for RNA cleavage by ribonuclease A (RNase A) (32). This suggests that general acid-base catalysis has the potential for providing enormous rate enhancements for ribozymes. Properly positioned cytosines and adenines could serve as general acids or bases in other ribozymes or enzymatic ribonucleoproteins. The catalytic repertoire of RNA and could allow RNA to catalyze other reactions, including peptide bond formation. Such features would enhance the ability of RNA to evolve and make the transition from an RNA world to a ribonucleoprotein world.

References and Notes

1. T. R. Cech and B. L. Golden, in *The RNA World*, R. F. Gesteland, T. R. Cech, J. F. Atkins, Eds. (Cold Spring Harbor Laboratory Press, Cold Spring Harbor, NY, ed. 2, 1999), pp. 321–349.
2. G. J. Narlikar and D. Herschlag, *Annu. Rev. Biochem.* **66**, 19 (1997).
3. W. P. Jencks, *Adv. Enzymol.* **43**, 219 (1975).
4. J. A. Piccirilli, J. S. Vyle, M. H. Caruthers, T. R. Cech, *Nature* **361**, 85 (1993); L. B. Weinstein, B. C. Jones, R. Cosstick, T. R. Cech, *Nature* **388**, 805 (1997); A. Yoshida, S. Sun, J. A. Piccirilli, *Nature Struct. Biol.* **6**, 318 (1999); S. Shan, A. Yoshida, S. Sun, J. A. Piccirilli, D. Herschlag, *Proc. Natl. Acad. Sci. U.S.A.* **96**, 12299 (1999).
5. A. Fersht, *Enzyme Structure and Mechanism* (Freeman, New York, ed. 2, 1985).
6. W. P. Jencks, in *Catalysis in Chemistry and Enzymology* (Dover, New York, 1987), pp. 163–242.
7. W. Saenger, *Principles of Nucleic Acid Structure*, C. R. Cantor, Ed. (Springer-Verlag, New York, 1984).
8. G. J. Connell and M. Y. Yarus, *Science* **264**, 1137 (1994).

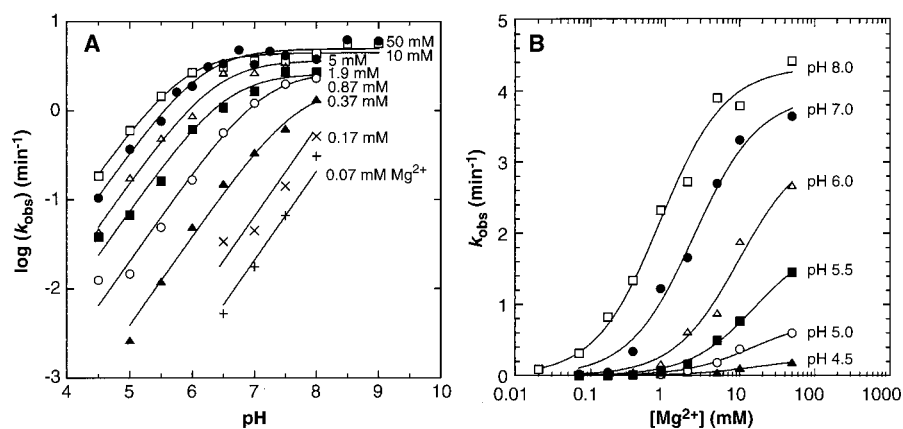


Fig. 5. (A) Reactivity-pH profiles for C75 in Mg^{2+} concentrations of 0.07 mM (+), 0.17 mM (x), 0.37 mM (\blacktriangle), 0.87 mM (\circ), 1.9 mM (\blacksquare), 5 mM (\triangle), 10 mM (\bullet), and 50 mM (\square). The Mg^{2+} concentrations have been corrected for the EDTA in the solution. Experiments were performed and analyzed as described in Fig. 3A. The observed pK_a values at 50, 10, 5, 1.9, 0.87, 0.37, 0.17, and 0.07 mM Mg^{2+} were 5.8, 6.1, 6.4, 6.5, 7.1, 7.7, ≥ 8 , and ≥ 8 , respectively. (B) Reactivity- Mg^{2+} profiles for C75 at pH 4.5 (\blacktriangle), pH 5.0 (\circ), pH 5.5 (\blacksquare), pH 6.0 (\triangle), pH 7.0 (\bullet), and pH 8.0 (\square). Experiments were performed as described in Fig. 3A. The Hill equation, $\log[k/(k_{\text{max}} - k)] = \Delta n_{\text{Mg}^{2+}} \log[\text{Mg}^{2+}] - \log K_{D,\text{Mg}^{2+}}$ (5), was used at each pH to determine $\Delta n_{\text{Mg}^{2+}}$, the number of functional magnesium ions that bind to the ribozyme. Plots of $\log[k/(k_{\text{max}} - k)]$ versus $\log[\text{Mg}^{2+}]$ yielded straight lines. The observed $\Delta n_{\text{Mg}^{2+}}$ values at pH 4.5, 5.0, 5.5, 6.0, 6.5 (not shown), 7.0, 7.5 (not shown), and 8.0 were 1.0, 1.6, 1.4, 1.3, 1.4, 1.4, 1.1, and 0.98, respectively, consistent with one functional magnesium ion binding in each pH condition. These plotted data were fit to the following binding equation for a single ion: $k_{\text{obs}} = k_{\text{max}}[\text{Mg}^{2+}]/(K_{D,\text{Mg}^{2+}} + [\text{Mg}^{2+}])$. The resulting observed $K_{D,\text{Mg}^{2+}}$ values at pH 4.5, 5.0, 5.5, 6.0, 6.5 (not shown), 7.0, 7.5 (not shown), and 8.0 were 16, 14, 16, 9.8, 3.1, 2.4, 1.2, and 0.86 mM, respectively.

9. P. Legault and A. Pardi, *J. Am. Chem. Soc.* **116**, 8390 (1994); *J. Am. Chem. Soc.* **119**, 6621 (1997).

10. A. T. Perrotta, I.-h. Shih, M. D. Been, *Science* **286**, 123 (1999).

11. M. D. Been and G. S. Wickham, *Eur. J. Biochem.* **247**, 741 (1997).

12. T. S. Wadkins, A. T. Perrotta, A. R. Ferré-D'Amaré, J. A. Doudna, M. D. Been, *RNA* **5**, 720 (1999).

13. A. R. Ferré-D'Amaré, K. Zhou, J. A. Doudna, *Nature* **395**, 567 (1998); A. R. Ferré-D'Amaré and J. A. Doudna, *J. Mol. Biol.* **295**, 541 (2000).

14. S. Nakano, D. M. Chadalavada, P. C. Bevilacqua, data not shown.

15. We confirmed that the C75U genomic ribozyme can be rescued by imidazole. In 10 mM Mg²⁺, pH 7.0, and 200 mM imidazole, an observed rate constant of 0.12 min⁻¹ was found.

16. K. R. Schowen and R. L. Schowen, *Methods Enzymol.* **87**, 551 (1982); J. H. Shim and S. J. Benkovic, *Biochemistry* **38**, 10024 (1999).

17. A. J. Kirby and M. Younas, *J. Chem. Soc. B*, 510 (1970); *J. Chem. Soc. B*, 1165 (1970); M. Oivanen, S. Kuusela, H. Lonnberg, *Chem. Rev.* **98**, 961 (1998).

18. D. Herschlag, F. Eckstein, T. R. Cech, *Biochemistry* **32**, 8312 (1993).

19. S. C. Dahm, W. B. Derrick, O. C. Uhlenbeck, *Biochemistry* **32**, 13040 (1993).

20. Y. A. Suh, P. K. Kumar, K. Taira, S. Nishikawa, *Nucleic Acids Res.* **21**, 3277 (1993).

21. A. Hampel and J. A. Cowan, *Chem. Biol.* **4**, 513 (1997); S. Nesbitt, L. A. Hegg, M. J. Fedor, *Chem. Biol.* **4**, 619 (1997); K. J. Young, F. Gill, J. A. Grasby, *Nucleic Acids Res.* **25**, 3760 (1997).

22. Dixon plots of $[k_{\text{obs}}(\text{min}^{-1})]^{-1}$ versus $[\text{Co}(\text{NH}_3)_6]^{3+}$, in 2 and 10 mM Mg²⁺, pH 7.0, yielded straight lines that intersect above the $[\text{Co}(\text{NH}_3)_6]^{3+}$ axis. This behavior is consistent with competitive inhibition, and revealed an inhibition constant K_i of $45 \pm 10 \mu\text{M}$ for $[\text{Co}(\text{NH}_3)_6]^{3+}$ [I. H. Segel, *Enzyme Kinetics* (Wiley, New York, 1993)]. The $K_{D, \text{Mg}^{2+}}$ at pH 7.0 is 2.4 mM (Fig. 5B). Tighter binding of $[\text{Co}(\text{NH}_3)_6]^{3+}$ may be due to electrostatic considerations. Similar relative affinities were noted for binding of these ions to the hairpin ribozyme [K. J. Hampel, N. G. Walter, J. M. Burke, *Biochemistry* **37**, 14672 (1998)]. Also, reaction in 10 mM $[\text{Co}(\text{NH}_3)_6]^{3+}$ was rescued by lowering the pH from 7.0 to 5.0 ($k_{\text{obs}} = 3.6 \times 10^{-3} \text{ min}^{-1}$) (14), as was the case with monovalent ions (Fig. 4A); this result supports native-like folding of the ribozyme in $[\text{Co}(\text{NH}_3)_6]^{3+}$.

23. R. Basolo and R. G. Pearson, *Mechanisms of Inorganic Reactions* (Wiley, New York, 1988); H. Suga, J. A. Cowan, J. W. Szostak, *Biochemistry* **37**, 10118 (1998).

24. J. H. Cate et al., *Science* **273**, 1678 (1996); J. H. Cate and J. A. Doudna, *Structure* **4**, 1221 (1996); J. H. Cate, R. L. Hanna, J. A. Doudna, *Nature Struct. Biol.* **4**, 553 (1997).

25. I.-h. Shih and M. D. Been, *RNA* **5**, 1140 (1999).

26. It has been suggested that the HDV ribozyme cannot be rescued by high concentrations of monovalent metal ions [J. B. Murray, A. A. Seyhan, N. G. Walter, J. M. Burke, W. G. Scott, *Chem. Biol.* **5**, 587 (1998)]. However, those authors reported a rate constant at pH 8 in the presence of 4 M Li⁺ and 25 mM EDTA, which is slower than that observed here (at pH 8.0 in the presence of 1 M Na⁺ and 1 mM EDTA) by a factor of only 3.6.

27. Because the transition state appears to be dominated by bond formation to the leaving group (17), the general base could be a poor base such as 55 M solvent water ($pK_a = -1.7$), a neighboring phosphate ($pK_a \sim 1$), or a ring nitrogen ($pK_a \sim 4$), which could partially deprotonate the 2'-hydroxyl in the transition state. Increasing the concentration of Hepes from 25 to 50 mM or that of EDTA from 1 to 2 mM did not affect the reaction rate in 1 M NaCl, which suggests that the buffer is not acting as the general base. Between pH 8 and 9, the profile is nearly independent of pH (Fig. 4A), which suggests that specific base catalysis by hydroxide ion may contribute in this regime.

28. V. K. Misra and D. E. Draper, *Biopolymers* **48**, 113 (1998).

29. B. W. Pontius, W. B. Lott, P. H. von Hippel, *Proc. Natl. Acad. Sci. U.S.A.* **94**, 2290 (1997).

30. F. da Silva and R. J. P. Williams, *The Biological Chemistry of the Elements* (Oxford Univ. Press, Oxford, 1993).

31. D. E. Schmidt Jr. and F. H. Westheimer, *Biochemistry* **10**, 1249 (1971).

32. The observed rate constant in saturating Mg²⁺ (50 mM) at pH 5.0 is 0.01 s⁻¹ (Fig. 5A). At pH 5.0, the fraction of C75 in the functional protonated state is ~1. The fraction of the magnesium ion in the functional unprotonated state is dependent on the pK_a of the ribozyme-bound $[\text{M}(\text{OH})]^+$ used in the calculation. The 50 mM Mg²⁺ data in Fig. 5A suggest that the pK_a for $[\text{Mg}(\text{H}_2\text{O})_6]^{2+}$ is >9, whereas the unperurbed pK_a of $[\text{Mg}(\text{H}_2\text{O})_6]^{2+}$ is 11.4 (19). Using the slope of 1 in Fig. 5A, the rate constant for chemistry is estimated at 10² to 10⁴ s⁻¹ ($\sim 0.01 \text{ s}^{-1} \times 10^{(pK_a-5)}$). The maximal cleavage rate for RNase A is $1.4 \times 10^3 \text{ s}^{-1}$ at 25°C [J. E. Thompson and R. T. Raines, *J. Am. Chem. Soc.* **116**, 5467 (1994)]. The rate constant for the chemical step in the *Tetrahymena* ribozyme has been estimated at 6 s⁻¹ at 50°C [D. Herschlag and T. R. Cech, *Biochemistry* **29**, 10159 (1990)].

33. D. Chadalavada, S. Knudsen, S. Nakano, P. C. Bevilacqua, in preparation.

34. A plasmid containing a T7 promoter and the template for the ribozyme was constructed by overlap extension and cloning into pUC19. Mutants were prepared using QuikChange (Stratagene). All DNA constructs were confirmed by dideoxy sequencing. The sequence for the ribozyme is based on a human isolate in which position 85 is a G [S. Makino et al., *Nature* **329**, 343 (1987)]. RNA was transcribed, gel-purified, and 5'-end-labeled by standard methods. RNA was renatured at 55°C for 10 min in 0.5 mM tris (pH 7.5) and 0.05 mM EDTA, then placed at room temperature for 10 min. A saturating concentration (10 μM final) of a DNA oligomer, AS1 [stored in 10 mM tris and 1 mM EDTA (pH 7.5)], which sequesters

an inhibitory stretch upstream of the cleavage site (33), was added, followed by addition of buffer. The buffer was 25 mM MES (for experiments at pH 4.5 to 6.5) or 25 mM Hepes (for experiments at pH 6.75 to 9.0). Similar kinetics were obtained upon adding small amounts of NaCl (50 mM) (pH 5.0 and 7.0) or changing the buffer to MOPS (pH 6.0 and 7.0) or BICINE (pH 8.0, 8.5, and 9.0). The experimental pH range was limited to 4.5 to 9.0 to avoid ionizing ring nitrogens with pK_a s outside of this range (7). Water used in the reactions was deionized by a Millipore system. The pH was determined at room temperature and corrected for the slight temperature dependence of buffer pK_a [N. E. Good et al., *Biochemistry* **5**, 467 (1966)]. This mixture was incubated at 37°C for 2 min, a zero time point was removed, and the reaction was initiated by addition of metal ions and performed at 37°C. Depending on the experiment, one of the following salts was added: MgCl₂, CaCl₂, CoCl₂, Co(NH₃)₆Cl₃, or NaCl and 1 mM EDTA. Selected reactions were also initiated by AS1 addition, and similar results were obtained. Quenching at various time points was done by addition of an equal volume of a solution of 20 mM EDTA and 90% formamide to $\leq 10 \text{ mM Mg}^{2+}$ solutions, or 100 mM EDTA and 90% formamide to 50 mM Mg²⁺ solutions, and the contents were immediately placed on dry ice. Reactions were separated on a 10% polyacrylamide gel containing 7 M urea, then quantitated on a PhosphorImager (Molecular Dynamics).

35. T. E. Ferrin, C. C. Huang, L. E. Jarvis, R. Langridge, *J. Mol. Graphics* **6**, 13 (1988).

36. Supported by NIH grant GM58709. We thank S. Benkovic, M. Bollinger, S. Booker, T. Glass, and members of the Bevilacqua lab for reading the manuscript before publication and for helpful comments, and S. Tan for assistance in preparing Fig. 3B.

16 November 1999; accepted 27 December 1999

Translocation of *Helicobacter pylori* CagA into Gastric Epithelial Cells by Type IV Secretion

Stefan Odenbreit, Jürgen Püls, Bettina Sedlmaier, Elke Gerland, Wolfgang Fischer, Rainer Haas*

The Gram-negative bacterium *Helicobacter pylori* is a causative agent of gastritis and peptic ulcer disease in humans. Strains producing the CagA antigen (*cagA*⁺) induce strong gastric inflammation and are strongly associated with gastric adenocarcinoma and MALT lymphoma. We show here that such strains translocate the bacterial protein CagA into gastric epithelial cells by a type IV secretion system, encoded by the *cag* pathogenicity island. CagA is tyrosine-phosphorylated and induces changes in the tyrosine phosphorylation state of distinct cellular proteins. Modulation of host cells by bacterial protein translocation adds a new dimension to the chronic *Helicobacter* infection with yet unknown consequences.

The Gram-negative bacterium *Helicobacter pylori* (*Hp*) colonizes the human gastric epithelium and is strongly associated with peptic ulceration, MALT-lymphoma, and adenocarcinoma of the stomach (1). The *cagA* gene is a genetic marker for a 40-kb pathogenicity island (*cag*-PAI) of *Hp*, present in certain strains (*cag*⁺, type I), but not in others (*cag*⁻, type II) (2). The function of the immunodominant CagA protein

is unknown. Attachment of *Hp* to epithelial cells in vitro induces tyrosine phosphorylation of a 145-kD host cell protein (3). Mutations in several genes of the *cag*-PAI interfere with tyrosine phosphorylation and secretion of the chemokine interleukin-8 (4, 5). The *cag*-PAI carries a set of genes with homology to so-called type IV secretion systems (6), the prototype of which is the *Agrobacterium tumefaciens*